2020 IEEE/RSJ International Conference on Intelligent Robots and Systems (IROS)
October 25-29, 2020, Las Vegas, NV, USA (Virtual)

Auditory Feedback Effectiveness for Enabling Safe Sclera Force in Robot-Assisted Vitreoretinal Surgery: a Multi-User Study

Ali Ebrahimi[1], Marina Roizenblatt[2,3], Niravkumar Patel[1] *Member, IEEE*
Peter Gehlbach[3] *Member, IEEE*, and Iulian Iordachita[1], *Senior Member, IEEE*

***Abstract*— Robot-assisted retinal surgery has become increasingly prevalent in recent years in part due to the potential for robots to help surgeons improve the safety of an immensely delicate and difficult set of tasks. The integration of robots into retinal surgery has resulted in diminished surgeon perception of tool-to-tissue interaction forces due to robot's stiffness. The tactile perception of these interaction forces (sclera force) has long been a crucial source of feedback for surgeons who rely on them to guide surgical maneuvers and to prevent damaging forces from being applied to the eye. This problem is exacerbated when there are unfavorable sclera forces originating from patient movements (dynamic eyeball manipulation) during surgery which may cause the sclera forces to increase even drastically. In this study we aim at evaluating the efficacy of providing warning auditory feedback based on the level of sclera force measured by force sensing instruments. The intent is to enhance safety during dynamic eye manipulations in robot-assisted retinal surgery. The disturbances caused by lateral movement of patient's head are simulated using a piezo-actuated linear stage. The Johns Hopkins Steady-Hand Eye Robot (SHER), is then used in a multi-user experiment. Twelve participants are asked to perform a mock retinal surgery by following painted vessels inside an eye phantom using a force sensing instrument while auditory feedback is provided. The results indicate that the users are able to handle the eye motion disturbances while maintaining the sclera forces within safe boundaries when audio feedback is provided.**

I. INTRODUCTION

After diabetic retinopathy, Retinal Vein Occlusion (RVO) has been reported to be the second most common retinal vascular disease among the elderly [1]. One of the possible clinical procedures to treat RVO is retinal vein cannulation (RVC) in which clot-dissolving tissue plasminogen activator (t-PA) is injected directly into the occluded vein [2] which has structures as small as 30 μm [3]. For an ophthalmic surgeon performing the surgical tasks, a root mean squared (RMS) of 38 μm was measured for tremor amplitude [4] which is a greater value compared to the retinal structures.

*This work was supported by U.S. National Institute of Health under grant number of 1R01EB023943-01 and Research to Prevent Blindness, New York, New York, USA, and gifts by the J. Willard and Alice S. Marriott Foundation, the Gale Trust, Mr. Herb Ehlers, Mr. Bill Wilbur, Mr. and Mrs. Rajandre Shaw, Ms. Helen Nassif, Ms Mary Ellen Keck, and Mr. Ronald Stiff.

[1]A. Ebrahimi, Niravkumar Patel, and I. Iordachita are with the Mechanical Engineering Department and Laboratory for Computational Sensing and Robotics (LCSR) at the Johns Hopkins University, Baltimore, MD, 21218, USA. E-mail: {aebrahi5, npatel89, iordachita}@jhu.edu

[2]M. Roizenblatt and P. Gehlbach are with the Wilmer Eye Institute, Johns Hopkins Hospital, Baltimore, MD 21287 USA. E-mail: maroizenb@gmail.com, pgelbach@jhmi.edu

[3]M. Roizenblatt is also with Federal University of São Paulo, São Paulo, 04023-062 Brazil.

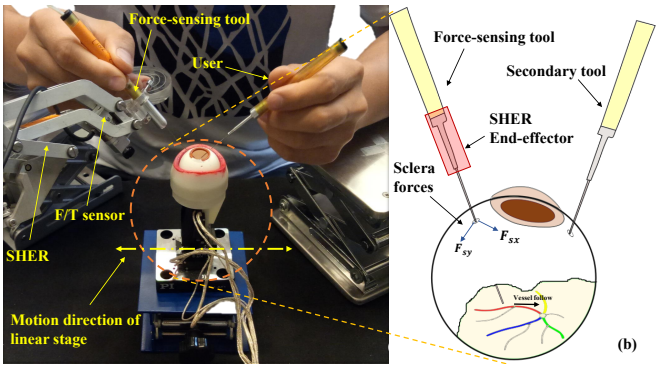

Fig. 1: Eye phantom manipulation with the SHER. (a) The surgeon is grabbing the force-sensing tool which is attached to the robot in the right hand and the secondary tool in the left hand to manipulate the eye phantom and to follow the vessels. (b) A schematic of following the vessels with tool tip is represented.

Therefore, the required skills to safely, consistently and efficiently perform such surgery is at the limit of human motor function. Procedures such as this and other therapeutic maneuvers in retinal microsurgery define it as one of the most delicate and complicated surgical disciplines.

Towards overcoming such hardships in retinal microsurgery and helping surgeons in terms of positioning accuracy and suppressing such involuntary hand-tremor, several robotic assisting methods have been developed over the past 20 years [5]. These robots can be broadly categorized into the three main groups of collaborative, tele-operated, and handheld systems. An example of a collaborative robotic system in which surgeon and robot share the control of surgical tools, is the SHER (Fig. 1-a) developed at the Johns Hopkins University [6]. A four-degree of freedom (DoF) novel collaborative robotic arm was also designed and fabricated by Gijbels et al. [7]. As far as tele-manipulated robot arms for eye surgery, several systems have been developed which are referenced in [8]–[13]. The clinical emergence of the robotic retinal surgery is attributed to recent studies by Edwards et al. [14] and Gijbels et al. [15] where they conducted the first robot-assisted eye surgeries on human patients. As an alternative to the table-mounted robotic systems, a magnetically-navigated system for subretinal injection [16] and an active tremor-cancelling hand-held device called Micron were also developed [17].

Although robots provide potential for tremor free and highly precise manipulation, the tool-to-eye interaction forces (sclera forces Fig. 1-b) will no longer be clearly perceived by surgeons. This basically occurs due to the large inertia and stiffness of robots relative to the small and

delicate sclera forces. If sclera forces increase in excess of safe boundaries, they pose serious risks on sclera tissue. In order to keep these forces in safe ranges during robot-assisted manipulations, various active and passive control algorithms have been implemented and tested. Ebrahimi et al. [18], [19] used adaptive control to actively modulate the unsafe sclera forces. Using deep learning, He et al. [20] predicted the unsafe sclera forces in advance and provided autonomous robotic actions to reduce the exceeding sclera forces [21]. Although these autonomous control schemes effectively maintain the sclera forces in safe ranges, robots autonomous interference may hamper the surgeons maneuver. Algorithms designed to provide less obtrusive control schemes include Cutler et al. [22] who conducted a multi-user experiment with clinicians and engineers and reported improved precision and safety during phantom membrane peeling when audio feedback for tool tip force was provided. Other studies also provided audio feedback from tool tip forces [23], [24] and tool insertion inside the eyeball [25]. Furthermore, multi-user studies to compare between robot-assisted and freehand retinal surgery procedures can be found in [26] and [27].

While to date studies of feedback resulting from tool tip forces propose promising results for enhanced safety, they have not utilized the sclera forces to provide auditory feedback. In a preliminary study, our group recently demonstrated that auditory feedback prevents excessive sclera forces when manipulating a static eyeball (eyeball fixed in an eye socket) using the SHER [28]. After assuring the effectiveness of audio feedback during static eye manipulations, we now aim to evaluate the efficiency of using sclera force-based auditory feedback for robot-assisted eye surgery during dynamic conditions with the patient head and eye are in motion (dynamic eyeball in contrary to static eyeball). We conduct a full-scale multi-user study by enrolling 12 participants (non-clinicians) who had no prior experience with the SHER. To simulate the effects of intra-operative patient head movement on sclera forces, a linear stage capable of flicking the eyeball is used. The users are asked to perform a mock retinal surgery with the SHER on a moving eyeball using a force sensing surgical instrument. Therefore, this study evaluates the provision of sclera force-based audio feedback for dynamic eye manipulation circumstances during robot-assisted eye surgery. To the best of our knowledge, this procedure, conducted through a multi-user study, has not been previously reported. In the following section, the components of the experimental setup and the experiment procedure are elaborated.

II. Materials and Methods

During retinal surgery the surgeon's wrists rest on a supporting wrist rest and the surgeon's hands rest on the patient's forehead. However, due to the patient's head movement during the surgery, there might be undesirable relative motions between the surgeon's hand and the patient's head leading to unwanted relative movement of the tool tip on retina that can be hazardous. In this study by integrating a piezo-actuated linear stage, we simulate such unwanted disturbances during

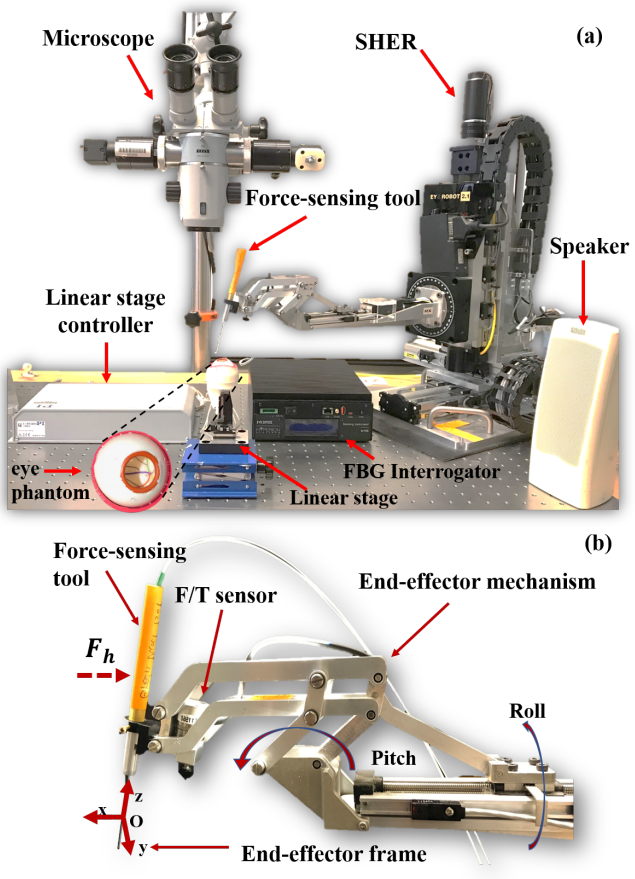

Fig. 2: (a) The experimental setup including the SHER, eye phantom, FBG interrogator, linear stage and its controller, microscope and speakers for providing audio feedback. (b) The close-up view for the SHER end-effector showing the place F_h is applied, the force sensing tool, and the two rotational degrees of freedom for the robot end-effector.

eye surgery. We intend to evaluate auditory feedback of sclera forces as a warning that may improve the patient safety in such circumstances.

A. The Steady-Hand Eye Robot

The SHER is a 5-DoF robot with 3 translating and 2 rotary DoFs (Fig. 2-b) which is designed and built at the Johns Hopkins University [29]. The robot works based on a collaborative control scheme where surgical tools are attached to the robot through a quick release mechanism. Surgeons share the tool handle with the robot and co-perform surgical tasks during near tremor free manipulations (Fig. 1-a).

There is a 6-DoF F/T sensor (Nano17, ATI Industrial Automation Inc., Apex, NC, USA) as shown in Fig. 2-b placed under the robot end-effector that is able to measure forces and torques $F_h \in \mathbb{R}^6$ as applied by user, in the end-effector coordinate frame (the frame is shown in Fig. 2-b). Then, the user interaction force is transferred to the robot base (fixed) coordinate frame using the forward kinematics of the robot. To obtain intuitive tool manipulation, the robot's admittance control scheme sets the desired translational and angular velocities of the end-effector frame, $\dot{X}_d \in \mathbb{R}^6$, to be proportional to F_h which is now expressed in the

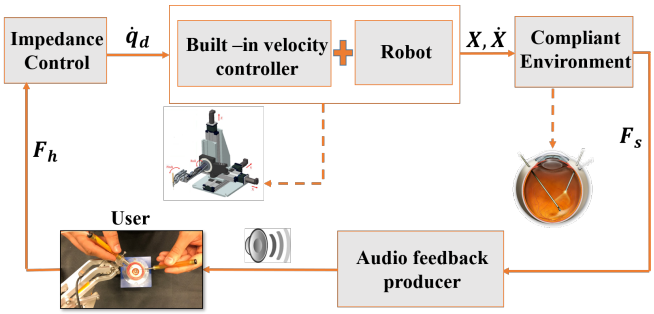

Fig. 3: Block diagram for the closed-loop system.

fixed coordinate frame. Therefore, the following equation describes the admittance control of the robot.

$$\dot{X}_d = \mathbb{K} F_h \tag{1}$$

where the first three elements of $\dot{X}_d$ represent the translational velocity of the origin of the end-effector frame (Fig. 2-b), and the last three elements of $\dot{X}_d$ are the angular velocity of end-effector frame expressed in the robot fixed frame. The matrix $\mathbb{K}$ is a constant diagonal matrix with positive entries on diagonal. Then, based on $\dot{X}_d$, the desired joint velocities $\dot{q}_d$ are found using the robot Jacobian pseudo inverse which gives the least-squares solution for $\dot{q}_d$.

$$\dot{q}_d = \underset{\dot{q}}{\operatorname{argmin}} \; ||\dot{X}_d - J(q)\dot{q}|| = J(q)^{\dagger}\dot{X}_d \tag{2}$$

where $J(q)$ is the robot Jacobian. Then, $\dot{q}_d \in \mathbb{R}^5$ is sent to the embedded velocity controller of the robot (Galil 4088, Galil, 270 Technology Way, Rocklin, CA 95765). The built-in joint velocity controller is able to move the joints based on $\dot{q}_d$.

B. Force-sensing tool

In order to detect and measure very small (tens of miliNewton) scleral forces between the tool shaft and the eyeball, a highly sensitive force sensor is required. In addition, the sensor should be incorporated into the thin shaft of the surgical tool. Fiber Bragg Grating (FBG) optical sensors (Technica S.A, Beijing, China), which are very sensitive strain sensors, can satisfy these requirements. The sensors are embedded into an optical fiber with a diameter of 80 μm. Each fiber has three active FBG zone which are depicted in Fig. 4-a. The active zones of the fibers (where there exist FBG sensors on the fibers) are denoted by FBG I, II and III in Fig. 4. Based on the reflected wavelength measured by an optical interrogator (sm130-700 from Micron Optics Inc., Atlanta, GA), which is shown in Fig. 2-a, we are able to calculate the tool shaft strain in each active zone.

As can be seen from Fig. 4, we designed a custom surgical needle by attaching three of the FBG fibers into the grooves carved at equal angular distances around the perimeter of the surgical needle shaft. This design is similar to what is suggested by [30]. Based on the details given in [30], by finding the relevant calibration matrices we are able to measure the sclera force, $F_s = \sqrt{F_{sx}^2 + F_{sy}^2}$ (F_{sx} and F_{sy} are the components of the sclera force in the end-effector frame as depicted in Fig. 1). After calibrating the tool, the RSME error for sclera force measurements was determined to be 1 mN.

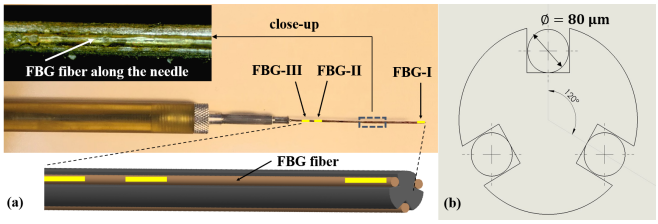

Fig. 4: Force-sensing tool. (a) Top view of the tool where FBG sensors are depicted with yellow line segments. (b) Cross section of the tool shaft showing three fibers each with diameter of 80 μm.

C. Auditory force feedback

To inform subjects of the sclera force level, audio feedback in the form of sound beeps were transmitted. The alarm beeps corresponded to the magnitude of sclera force, which are measured by the FBG sensors. We chose the beep thresholds based on a qualitative analysis derived from a retinal surgeon manipulating a phantom eyeball [28]. In that analysis, we asked an expert surgeon to perform freehand (without a robot) eye manipulations in a clinically relevant task. Then, we collected the sclera force information for the surgeon based on which we came up with 120 mN as the upper safe boundary for sclera force. This is a number that we obtained by averaging the force data recorded from our expert surgeon. In other words, this is a hypothetical value that we are using in the current experiments and does not necessarily mean that forces above this value will harm the actual sclera tissue.

To gradually warn subjects about approaching this unsafe level, we designed three levels of noises sounded by a speaker placed next to the subject (Fig. 2-a). When the sclera force (F_s) was < 80 mN, the speaker is silent. For sclera forces between 80 mN and 100 mN the first level alarm is emitted. For forces between 100 mN and 120 mN in which the subject is reaching the upper safe limit, another noise with higher frequency and volume is played. Finally, when subjects exceed the safe manipulation level, a high-pitch tone with a high volume is played in a continuous way to notify the subject about the excessive level of sclera force. The block diagram of the closed-loop system is depicted in Fig. 3.

D. Eye Phantom and Linear Stage

To simulate the retinal surgery environment, an artificial eye phantom has been made out of silicon with an inner diameter of 25 mm which is the average length for human eyeball (Fig. 2-a). To simulate the disturbances coming from patient head motion, we chose a piezo-actuated linear stage (Q-Motion Stages with the controller model E-873.3QTU - Physik Instrumente (PI) GmbH & Co. KG) to create lateral motions for the eyeball (Fig. 1-a). An eye socket was 3D-printed to enable the eyeball to be attached to the linear stage. Mineral oil was used to lubricate the surface between the eyeball and inside the socket. We also placed four painted vessels on the phantom retina to follow them during the experiment (Fig. 1-b).

The linear stage has the maximum range of 6 mm for each of its three Cartesian axis (Fig. 1-a). During cataract surgery, the mean value for lateral head drift was reported 2.9 mm [31]. In some extreme cases the operating microscope had to be adjusted to accommodate the head drift. In order to simulate lateral movements of patient's head, we programmed a stage supporting the phantom to produce a harmonic motion with an amplitude of 1 mm in the direction shown in Fig. 1-a (1-DoF simulation of eyeball motion). This amplitude did not require us to move the microscope during the experiments. Of note, the continuing harmonic motion is just to stimulate the users to react to them and to evaluate the effectiveness of providing audio feedback in our experiments. In other words, patient head motion, which occasionally happens during a real surgery, is not in the form of harmonic motion.

The linear stage is able to produce motion with a finite number of different frequencies (velocities) to create the harmonic motion. We conducted an experiment aiming at assessing different velocities of the stage. These experiments were performed by a single subject (experienced with the SHER). The results were analyzed to see what the effects of different velocities of the linear stage might be on safety of eye manipulation. In other words, we wanted to see with what velocities the audio feedback would be useful and the experienced user would still be able to catch up with the stage motion. We came up with six different velocities (Table I) for harmonic motion of the stage and one user performed the fourth step mentioned in section II-F for all of these six velocities.

Totally, six sets of experiments were conducted with the robot and each of the experiments was repeated five times. We performed two different analysis on the results obtained from this part: 1) Force derivative analysis and 2) Frequency response analysis which are explained as follows.

1) Force derivative analysis: The time derivative of sclera force is a measure of impact forces applied to the sclera. Forces applied in impact form can be more harmful than those applied smoothly even when their magnitude is identical. To observe the effect of stage velocity on the derivative of the sclera force, we calculated the average of all absolute values of sclera force derivative for each stage velocity experiment. The results are shown in Fig. 5. As it is obvious, the average derivative of sclera force increases as the stage velocity is increased. The experienced subject was not able to control the impact of sclera force in higher velocities of the stage, although audio feedback was provided. Actually,

TABLE I: Values for stage velocity during the velocity analysis experiments.

	Time period for one complete cycle (s)	Frequency (Hz)	Corresponding average velocity (mm/s)
Velocity 1	0 (steady eye)	-	0
Velocity 2	1.53	0.65	1.3
Velocity 3	1.15	0.87	1.73
Velocity 4	0.89	1.12	2.2
Velocity 5	0.75	1.3	2.6
Velocity 6	0.62	1.6	3.2

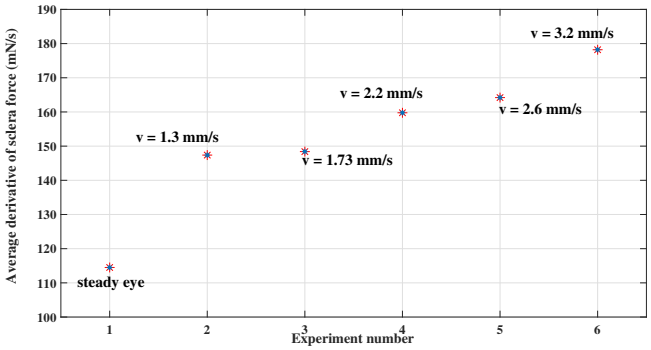

Fig. 5: Average of sclera force derivative in robot-assisted experiments for different values of stage velocities.

in high velocities (upper than 1.3 mm/s and 1.73 mm/s) the motion of the stage was too fast to be controlled by the audio feedback.

2) Frequency response analysis: The other analysis that we performed was the Fourier Transform of the sclera forces for each velocity of the stage. As mentioned earlier, each robot-assisted experiment for velocity analysis experiment was repeated five times. For each trial we executed the Fourier Transform and then we averaged the Fourier Transform results for all of the trials within each stage velocity. The results are shown in Fig. 6. As it is observed from Fig. 6, in velocities more than 1.3 mm/s a peak is produced around the corresponding frequency of the stage for that plot. The peak is barely seen in the velocity of 1.73 mm/s and in other words the velocity 1.73 mm/s is at the edge of producing a peak. For the velocities more than 1.73 mm/s the peak in the frequency response can be easily seen. These peaks indicate that the experienced user is not able to handle the safety of sclera force and catch up with the stage velocity even when the audio feedback is provided. The tool shaft keeps colliding the eyeball with the same frequency of the stage motion resulting in producing such peaks in the frequency response. Therefore, based on the discussions in sections II-D.1 and II-D.2, it seems that the velocity 1.3 mm/s is in the margin of safe manipulation and is potentially able to be handled with the audio feedback. The multi-user experiments were conducted with this velocity (velocity2 in Table I) of the linear stage.

E. Human Subjects

After attaining the approval from the Johns Hopkins University Institutional Review Board we looked for volunteers (older than 18) with no known motor or hearing disabilities to participate in this research study. We enrolled twelve engineers all affiliated with the Johns Hopkins University who signed a written, informed consent before conducting the experiments. The subjects were novice at the experiments and had never experienced such activities beforehand, so we would be able to evaluate the performance of the system using unbiased users.

F. Experiment procedure

Step one was a detailed explanation to each user. During the experiment, the subjects held two surgical tools in their hand, but only one of the tools had force sensing capabilities

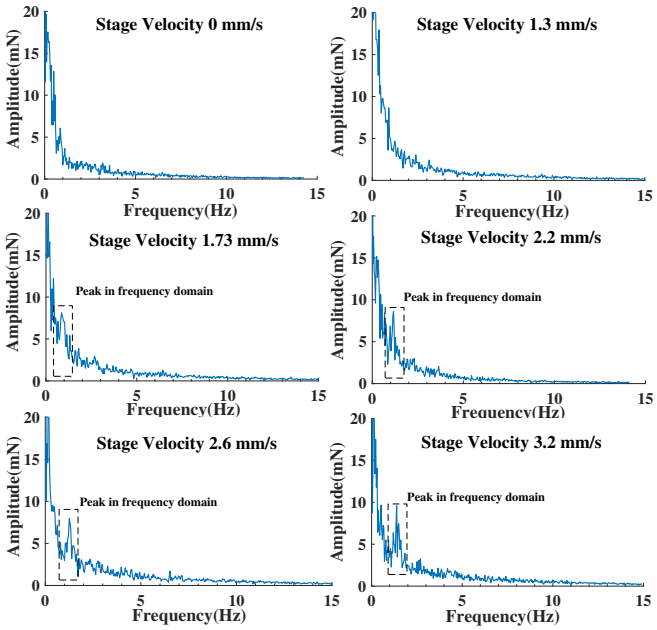

Fig. 6: Spectrum of sclera force in frequency domain for different velocities of the linear stage in robot-assisted cases.

with FBG sensors on it (Fig. 1). The other tool was just a simple surgical instrument that could not measure sclera forces. The subjects held the smart tool (force sensing tool) with their dominant hand. The subjects were asked to respond to audio feedback and to use that to maintain the level of sclera force in safe zones. All of the subjects went through a few minutes training to obtain an intuitive feeling about how to deal with the robot and how to react to lower the sclera force when the beep level was rising.

Following training, in each trial the subjects were given a random sequence of four colors of vessels and were asked to follow them with the force-sensing tool tip (Fig. 1-b) while looking through the microscope shown in Fig. 2-a. The subjects were supposed to keep the tool tip as close as possible to the vessels, but not to touch them while following the vessels. There were totally four conditions for the experiments as follows:

1) Freehand with audio feedback with steady stage (5 trials)
2) Freehand with audio feedback with moving stage (5 trials)
3) Robot-assisted with audio feedback with steady stage (5 trials)
4) Robot-assisted with audio feedback with moving stage (5 trials)

Each participant was asked to repeat each condition for 5 trials with a new random sequence of vessel colors.

III. Results

During the experiments, sclera force components and time information for all experiments were recorded using a software package [22] for controlling the SHER, developed using the C++ CISST-SAW libraries [32]. The recorded data were then analyzed using MATLAB (Mathworks Inc. , Natick, MA, USA).

TABLE II: Average time data for the multi-user experiments. The numbers in parenthesis indicates the standard deviation.

	Total Time (s)	Total time above 120 mN (s)	Time percentage spent over 120 mN
Freehand – Steady eye	42.7 (8.89)	4.98 (3.23)	11.7 %
Freehand – Moving eye	35.56 (5.91)	3.82 (1.98)	10.7 %
Robot – Steady eye	59.42 (15.18)	16.41 (6.55)	27.6 %
Robot – Moving eye	49.29 (8.15)	15.19 (5.76)	31.0v%

Table II and Table III present the results averaged over all of the 12 subjects taking part in the experiments. The tables include the force and time data associated with the experiments. Table II represents the total time required to accomplish all four conditions averaged for all users. As discussed in section II-C, the upper safe limit for eye manipulation was set at 120 mN. In order to realize how safe each specific task (condition) has been performed, we have averaged out the time spent at the forces greater than 120 mN for each of the tasks over all users and the results are written in Table II .

Table III represents the sclera force information measured during the experiments. This table includes the magnitude of sclera forces averaged over all users during each of the four tasks. In addition the averaged mode of sclera force has also been provided in Table III. The mode of sclera force refers to the most frequent sclera force during each maneuver. To calculate this value, we divided the sclera force range into equal segments with the lengths of 10 mN. Then, the middle point of the segment for which most of the manipulation time has been spent in that range represents the mode of sclera force for that specific task.

Boxplots for sclera force, total time and the total time spent on forces more than 120 mN are plotted in Figs. 7, 8 and 9, respectively. To do this, first all data from all users are categorized according to each of the four main experiments (explained in section II-F), and then the boxplots are plotted for all data in each of these categories.

At the end of each experiment for each user, a questionnaire was provided and the users were asked which of the four conditions better helped in completing the task. Nine of the users answered to this question based on a scale from 1 (very good) to 5 (very bad). Error bars for the users response to the questionnaire are provided in Fig. 10.

TABLE III: Average sclera force data for the multi-user experiments. The numbers in parenthesis indicates the standard deviation.

	Mode of sclera force (mN)	Average sclera force (mN)
Freehand – Steady eye	**58.25**	**70.19 (37.55)**
Freehand – Moving eye	**45**	**65.17 (35.98)**
Robot – Steady eye	**69.67**	**102.73 (59.01)**
Robot – Moving eye	**58.58**	**102.4 (62.84)**

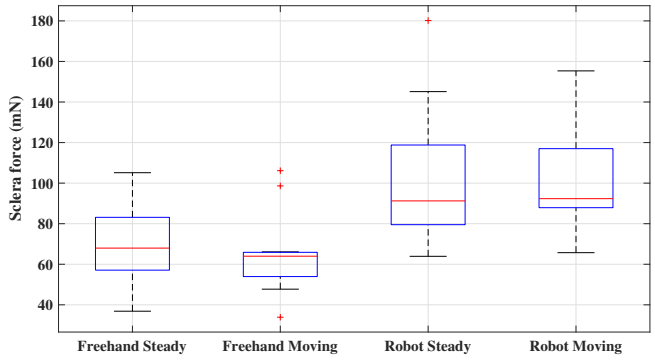

Fig. 7: Boxplot for sclera force for the results averaged out for all users over each task.

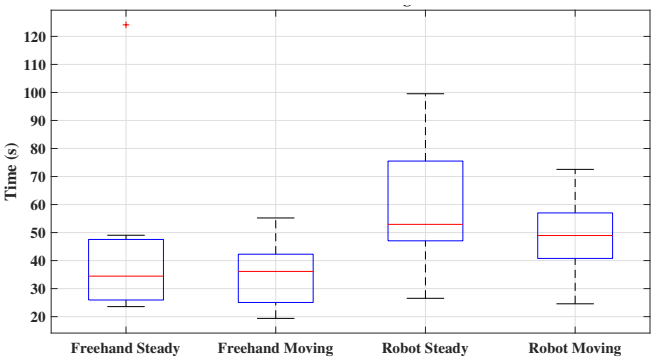

Fig. 8: Boxplot for total time for the results averaged out for all users over each task.

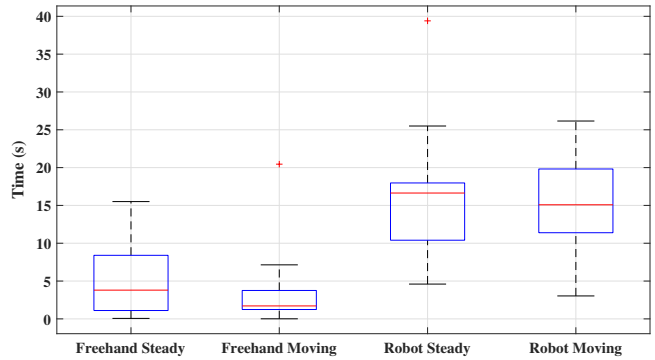

Fig. 9: Boxplot for time spent on forces more than 120 mN for the results averaged out for all users over each task.

IV. Discussion and Conclusion

In order to make statistically relevant conclusions, Student t tests are performed using Stata statistical software version 15.0, and p-values are obtained which are explained as follows. Tables II documents that the average time spent with unsafe scleral forces (more than 120 mN) for the tasks done with freehand are much less than those with the robot (p-value < 0.001). A similar behavior is observed for the ratio of the unsafe time to the total time which is provided in the fourth column of Tables II. After looking into Table III and comparing the average values for sclera force during robot-assisted tasks and freehand tasks, this conclusion will be further verified (all p-values < 0.001). This observation is in line with what was anticipated that sclera forces are higher during a robot-assisted eye surgery and sclera tissue safety is of more importance. In other words, although auditory feedback generated form the sclera force was provided to

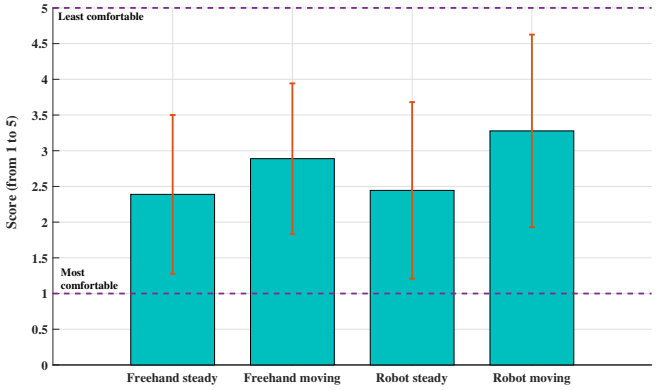

Fig. 10: Error bars for the questionnaire asked from users. Nine of the users contributed in this questionnaire.

the users in all of the robot-assisted task, the users were not able to maintain the sclera force at safe levels as well as the freehand manipulation.

Considering Tables II and III, it can be observed that for the moving eye tasks the users were able to keep the sclera forces and also time spent at unsafe forces at the same level as those seen in the static eye for that category (freehand or robot-assisted). For instance, the average value of sclera force for freehand steady eye and freehand moving eye tasks are 70.19 mN and 65.17 mN, respectively. These values for the robot-assisted tasks are 102.73 mN and 102.4 mN. After doing t test for sclera forces for these cases, p-values of 0.3 and 0.8 were obtained between moving and steady eye conditions in freehand and robot-assisted categories, respectively. Based on these p-values, we realized there is not any significant difference between the sclera forces of the moving and steady eye cases during freehand and robot-assisted manipulations. In other words, the auditory feedback is sufficient to help the users to keep the sclera forces in the moving eye tasks as safe as steady eye tasks. The same scenario is happening for the time spent on forces more than 120 mN where p-values of 0.3 and 0.5 were obtained between moving and static eye during freehand and robot-assisted manipulations, respectively. By looking into Figs. 7 and 9 consistent conclusions can be made. Figs. 7 and 9 indicate that the boxes attributed to robot-assisted conditions (steady and moving eyeball) are in similar range. Similarly, the median (red lines in Figs. 7 and 9) for freehand boxplots (steady and moving eyeball) are close to each other.

After doing a t test on the results of the questionnaire (Fig. 10) we could not reject the null hypothesis with significance level of 5%. The null hypothesis is to have equal means for scores for all of the four different tasks. In other words, the users on average did not have any comfort preference in performing the freehand or robotic manipulation.

To sum up, in this study we evaluated the effect of providing auditory feedback on enhancing sclera force safety during robot-assisted retinal surgery. The auditory feedback was assessed during static and dynamic eye manipulations, which simulates patient head motion during the surgery. Based on the results obtained from multi-user study with 12 participants, we can conclude that the auditory feedback is sufficient for handling the dynamic eye situations, and the

users were able to keep the sclera forces as safe as static eye case if the audio feedback was provided.

The future work of this study is to combine the audio feedback method and the autonomous control methods resulting in less intervening and safer control strategies.

REFERENCES

[1] J. Rehak and M. Rehak, "Branch retinal vein occlusion: pathogenesis, visual prognosis, and treatment modalities," *Current eye research*, vol. 33, no. 2, pp. 111–131, 2008.

[2] J. N. Weiss and L. A. Bynoe, "Injection of tissue plasminogen activator into a branch retinal vein in eyes with central retinal vein occlusion," *Ophthalmology*, vol. 108, no. 12, pp. 2249–2257, 2001.

[3] T. Meenink, G. Naus, M. de Smet, M. Beelen, and M. Steinbuch, "Robot assistance for micrometer precision in vitreoretinal surgery," *Investigative ophthalmology & visual science*, vol. 54, no. 15, pp. 5808–5808, 2013.

[4] S. Singh and C. Riviere, "Physiological tremor amplitude during retinal microsurgery," in *Proceedings of the IEEE 28th Annual Northeast Bioengineering Conference (IEEE Cat. No. 02CH37342)*. IEEE, 2002, pp. 171–172.

[5] R. Channa, I. Iordachita, and J. T. Handa, "Robotic eye surgery," *Retina (Philadelphia, Pa.)*, vol. 37, no. 7, p. 1220, 2017.

[6] B. Mitchell, J. Koo, I. Iordachita, P. Kazanzides, A. Kapoor, J. Handa, G. Hager, and R. Taylor, "Development and application of a new steady-hand manipulator for retinal surgery," in *Robotics and Automation, 2007 IEEE International Conference on*. IEEE, 2007, pp. 623–629.

[7] A. Gijbels, N. Wouters, P. Stalmans, H. Van Brussel, D. Reynaerts, and E. Vander Poorten, "Design and realisation of a novel robotic manipulator for retinal surgery," in *Intelligent Robots and Systems (IROS), 2013 IEEE/RSJ International Conference on*. IEEE, 2013, pp. 3598–3603.

[8] J. T. Wilson, M. J. Gerber, S. W. Prince, C.-W. Chen, S. D. Schwartz, J.-P. Hubschman, and T.-C. Tsao, "Intraocular robotic interventional surgical system (iriss): Mechanical design, evaluation, and master–slave manipulation," *The International Journal of Medical Robotics and Computer Assisted Surgery*, vol. 14, no. 1, p. e1842, 2018.

[9] W. Wei, R. Goldman, N. Simaan, H. Fine, and S. Chang, "Design and theoretical evaluation of micro-surgical manipulators for orbital manipulation and intraocular dexterity," in *Robotics and Automation, 2007 IEEE International Conference on*. IEEE, 2007, pp. 3389–3395.

[10] M. A. Nasseri, M. Eder, S. Nair, E. Dean, M. Maier, D. Zapp, C. P. Lohmann, and A. Knoll, "The introduction of a new robot for assistance in ophthalmic surgery," in *2013 35th Annual International Conference of the IEEE Engineering in Medicine and Biology Society (EMBC)*. IEEE, 2013, pp. 5682–5685.

[11] Z. Li, M. Shahbazi, N. Patel, E. O. Sullivan, H. Zhang, K. Vyas, P. Chalasani, A. Deguet, P. L. Gehlbach, I. Iordachita *et al.*, "Hybrid robotic-assisted frameworks for endomicroscopy scanning in retinal surgeries," *arXiv preprint arXiv:1909.06852*, 2019.

[12] S. Tanaka, K. Harada, Y. Ida, K. Tomita, I. Kato, F. Arai, T. Ueta, Y. Noda, N. Sugita, and M. Mitsuishi, "Quantitative assessment of manual and robotic microcannulation for eye surgery using new eye model," *The International Journal of Medical Robotics and Computer Assisted Surgery*, vol. 11, no. 2, pp. 210–217, 2015.

[13] C. He, L. Huang, Y. Yang, Q. Liang, and Y. Li, "Research and realization of a master-slave robotic system for retinal vascular bypass surgery," *Chinese Journal of Mechanical Engineering*, vol. 31, no. 1, p. 78, 2018.

[14] T. Edwards, K. Xue, H. Meenink, M. Beelen, G. Naus, M. Simunovic, M. Latasiewicz, A. Farmery, M. de Smet, and R. MacLaren, "First-in-human study of the safety and viability of intraocular robotic surgery," *Nature Biomedical Engineering*, p. 1, 2018.

[15] A. Gijbels, J. Smits, L. Schoevaerdts, K. Willekens, E. B. Vander Poorten, P. Stalmans, and D. Reynaerts, "In-human robot-assisted retinal vein cannulation, a world first," *Annals of Biomedical Engineering*, pp. 1–10, 2018.

[16] S. L. Charreyron, Q. Boehler, A. Danun, A. Mesot, M. Becker, and B. J. Nelson, "A magnetically navigated microcannula for subretinal injections," *IEEE Transactions on Biomedical Engineering*, 2020.

[17] C. N. Riviere, W. T. Ang, and P. K. Khosla, "Toward active tremor canceling in handheld microsurgical instruments," *IEEE Transactions on Robotics and Automation*, vol. 19, no. 5, pp. 793–800, 2003.

[18] A. Ebrahimi, N. Patel, C. He, P. Gehlbach, M. Kobilarov, and I. Iordachita, "Adaptive control of sclera force and insertion depth for safe robot-assisted retinal surgery," in *2019 International Conference on Robotics and Automation (ICRA)*. IEEE, 2019, pp. 9073–9079.

[19] A. Ebrahimi, F. Alambeigi, I. E. Zimmer-Galler, P. Gehlbach, R. H. Taylor, and I. Iordachita, "Toward improving patient safety and surgeon comfort in a synergic robot-assisted eye surgery: A comparative study," in *2019 IEEE/RSJ International Conference on Intelligent Robots and Systems (IROS)*. IEEE, 2019, pp. 7075–7082.

[20] C. He, N. Patel, I. Iordachita, and M. Kobilarov, "Enabling technology for safe robot-assisted retinal surgery: Early warning for unsafe scleral force," in *Robotics and Automation (ICRA), 2019 IEEE International Conference on*. IEEE, 2019.

[21] C. He, N. Patel, M. Shahbazi, Y. Yang, P. L. Gehlbach, M. Kobilarov, and I. Iordachita, "Toward safe retinal microsurgery: development and evaluation of an rnn-based active interventional control framework," *IEEE Transactions on Biomedical Engineering*, 2019.

[22] N. Cutler, M. Balicki, M. Finkelstein, J. Wang, P. Gehlbach, J. McGready, I. Iordachita, R. Taylor, and J. T. Handa, "Auditory force feedback substitution improves surgical precision during simulated ophthalmic surgery," *Investigative ophthalmology & visual science*, vol. 54, no. 2, pp. 1316–1324, 2013.

[23] M. Balicki, A. Uneri, I. Iordachita, J. Handa, P. Gehlbach, and R. Taylor, "Micro-force sensing in robot assisted membrane peeling for vitreoretinal surgery," in *International Conference on Medical Image Computing and Computer-Assisted Intervention*. Springer, 2010, pp. 303–310.

[24] B. Gonenc, J. Handa, P. Gehlbach, R. H. Taylor, and I. Iordachita, "A comparative study for robot assisted vitreoretinal surgery: micron vs. the steady-hand robot," in *2013 IEEE International Conference on Robotics and Automation*. IEEE, 2013, pp. 4832–4837.

[25] S. Matinfar, M. A. Nasseri, U. Eck, H. Roodaki, N. Navab, C. P. Lohmann, M. Maier, and N. Navab, "Surgical soundtracks: Towards automatic musical augmentation of surgical procedures," in *International Conference on Medical Image Computing and Computer-Assisted Intervention*. Springer, 2017, pp. 673–681.

[26] M. F. Jacobsen, L. Konge, M. Alberti, M. la Cour, Y. S. Park, and A. S. S. Thomsen, "Robot-assisted vitreoretinal surgery improves surgical accuracy compared with manual surgery: A randomized trial in a simulated setting," *RETINA*, 2020.

[27] T. Ueta, T. Nakano, Y. Ida, N. Sugita, M. Mitsuishi, and Y. Tamaki, "Comparison of robot-assisted and manual retinal vessel microcannulation in an animal model," *British Journal of Ophthalmology*, vol. 95, no. 5, pp. 731–734, 2011.

[28] A. Ebrahimi, C. He, M. Roizenblatt, N. Patel, S. Sefati, P. Gehlbach, and I. Iordachita, "Real-time sclera force feedback for enabling safe robot-assisted vitreoretinal surgery," in *2018 40th Annual International Conference of the IEEE Engineering in Medicine and Biology Society (EMBC)*, July 2018, pp. 3650–3655.

[29] A. Üneri, M. A. Balicki, J. Handa, P. Gehlbach, R. H. Taylor, and I. Iordachita, "New steady-hand eye robot with micro-force sensing for vitreoretinal surgery," in *Biomedical Robotics and Biomechatronics (BioRob), 2010 3rd IEEE RAS and EMBS International Conference on*. IEEE, 2010, pp. 814–819.

[30] X. He, M. Balicki, P. Gehlbach, J. Handa, R. Taylor, and I. Iordachita, "A multi-function force sensing instrument for variable admittance robot control in retinal microsurgery," in *Robotics and Automation (ICRA), 2014 IEEE International Conference on*. IEEE, 2014, pp. 1411–1418.

[31] K. Brogan, B. Dawar, D. Lockington, and K. Ramaesh, "Intraoperative head drift and eye movement: two under addressed challenges during cataract surgery," *Eye*, vol. 32, no. 6, p. 1111, 2018.

[32] P. Kazanzides, Z. Chen, A. Deguet, G. S. Fischer, R. H. Taylor, and S. P. DiMaio, "An open-source research kit for the da vinci® surgical system," in *2014 IEEE international conference on robotics and automation (ICRA)*. IEEE, 2014, pp. 6434–6439.